ACS APPLIED MATERIALS & INTERFACES

Research Article

www.acsami.org

Sunlight-Induced Synthesis of Various Gold Nanoparticles and Their Heterogeneous Catalytic Properties on a Paper-Based Substrate

Jun-Hyun Kim,*[,†] Katrina M. Twaddle,[†] Jiayun Hu,[†] and Hongsik Byun*[,‡]

[†]Department of Chemistry, Illinois State University, Normal, Illinois 61790-4160, United States

[‡]Department of Chemical System Engineering, Keimyung University, Daegu, 704-701, South Korea

Supporting Information

ABSTRACT: This work describes the light-induced preparation of various gold nanoparticles and demonstrates their possible use as efficient photothermal heating materials and practical heterogeneous catalysts under the irradiation of a solar-based light after being loaded onto a paper-based substrate. The synthesis of gold nanoparticles was accomplished under the irradiation of daily sunlight and a solar-simulated light with an intensity that was closely adjusted to the one-sun condition. Tunable sizes of gold nanoparticles were systematically controlled by the ratio of trisodium citrate and gold chloride ions, particularly with the solar-simulated light source. The size distribution and absorption properties of the resulting nanoparticles were thoroughly characterized by scanning electron microscope, dynamic light scattering, and UV−visible spectroscopy. The broad-band solar-based light sources were found to be efficient external stimuli to induce/enhance the formation of various gold nanoparticles at room temperature. As gold nanoparticles typically exhibit efficient light-induced heating properties due to their strong absorption bands, these nanoparticles were physically embedded on a filter paper to examine their photothermal heating properties and heterogeneous catalytic activity in the reduction of 4-nitrophenol under the irradiation of the solar-simulated light. As expected, the gold-loaded filter papers exhibited a systematic increase of temperature as a function of the gold nanoparticle concentration and enhanced catalytic property under the irradiation of the light, presumably caused by the photothermally induced heating property of the loaded gold nanoparticles. Overall, solar-based light sources can offer dual functions for the synthesis and application of metal nanoparticles possessing strong absorption bands.

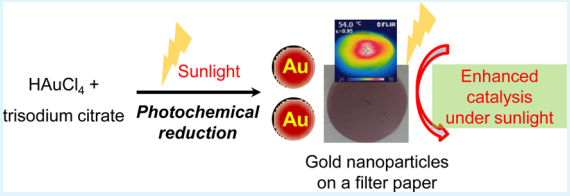

KEYWORDS: *sunlight, photothermal heating, heterogeneous catalysis, filter paper, gold nanoparticles*

1. INTRODUCTION

Nanoscale colloidal metal particles have been widely studied due to their optical, electrical, and catalytic properties, along with their biocompatible nature.[1−5] Gold nanoparticles can particularly exhibit absorption coefficients of five or higher orders of magnitude than typical molecular chromophores,[6] and their absorption properties (i.e., surface plasmon resonance, SPR) have been modified and intensified as a function of the gold structures (e.g., size and shape).[4,5,7−10] In addition, one useful feature of gold nanoparticles is their structure-dependent photothermal heating property, in other words, the ability to absorb light and release the absorbed light energy in the form of heat (photon-to-heat conversion property),[8,11−16] which makes these types of metal nanoparticles fascinating optical materials. Thus, methods for the controlled synthesis of various gold nanoparticles are being extensively investigated since the ability to tune both their optical and photothermal heating properties may be relevant to numerous applications.[7,10,12,13,17−19] Our group previously demonstrated the simple light-induced synthetic strategy for preparing gold nanoparticles that allowed for reasonable success of controlling particle size at room temperature.[20] A further refinement of our method could be achieved by utilizing solar-based broad-band light sources and may lead to advancements in designing new metallic nanoparticles. The prepared nanoparticles can then be loaded onto a paper-based substrate to exhibit the light-induced heating property and heterogeneous catalytic activity under a solar-simulated light source; this application of gold nanoparticles may be developed into highly practical, inexpensive, and environmentally friendly heating devices and catalytic systems.

The trisodium citrate-based thermal reduction is a common approach for preparing various gold nanoparticles ranging from 15 to 147 nm possessing strong SPRs.[12,13,21] Although this preparation method simply involves controlling the ratios of citrate to gold ions,[12,17,22−24] the reaction often needs to be carried out on a relatively large scale at the temperature of boiling water and lacks the reproducible preparation of large uniform gold nanoparticles. On the basis of our previous study, the photochemical synthetic method could result in the reliable preparation of monodispersed gold nanoparticles with tunable size ranges (∼15−75 nm in diameter) at room temperature on a small scale (≤10 mL) under the irradiation of visible light.[20] As such, we attempted to further improve the photochemical

Received: April 10, 2014
Accepted: June 18, 2014
Published: July 1, 2014

reaction method on a small scale at room temperature by utilizing broad-band light sources (i.e., solar-simulated light and sunlight) to prepare the tunable sizes of gold nanoparticles possessing intense absorption bands. This light-induced preparation process presumably involves the relatively slow formation of a trace amount of gold atoms and clusters at the early stages in the presence of trisodium citrate, which leads to the formation of small gold nanoparticles. It is followed by the greatly increased reduction rate of gold ions around these small nanoparticles due to their strong enough absorption band (520−550 nm) under visible light irradiation causing the autocatalytic growth process. As such, the use of broad-band light sources (e.g., solar-based light) in the photochemical method could provide an alternative reaction process to prepare a wider size range of gold nanoparticles and fulfill some of the drawbacks of the other synthetic methods. Our successful synthetic approach could generalize the preparation of other types of nanoparticles possessing strong SPRs under renewable light sources, allowing for their practical applications in nanoscience and technology.

To utilize the prepared gold nanoparticles possessing strong SPRs in the visible range, these nanoparticles were embedded on paper-based substrates, which were then exposed to a solar-simulated light to obtain photothermally induced heating measurements as a function of the concentration of the gold nanoparticles. As these gold-nanoparticle-loaded filter papers exhibited significant light-induced heating caused by the efficient absorption of the broad-band incident light, these systems were employed in the catalytic reduction of 4-nitrophenol (4-NP) under the irradiation of the solar-simulated light. It is noted that many catalytic reactions could result in improved yields at an increased reaction temperature,[25−28] and our catalytic system which utilizes the photothermal heating capability of gold nanoparticles can afford notable enhancements of the reduction process under light irradiation. Employing these optically active gold nanoparticles on a paper-based substrate can serve as a simple heterogeneous catalyst that will lead to the development of photothermally enhanced catalytic systems. A thorough examination of the relationship between the absorption property (i.e., SPR) and photothermal heating efficiency of gold nanoparticles is underway in order to improve the photoenhanced chemical reaction systems or related applications.[6,29−33] Use of paper-based materials will also allow for designing practical, low-cost, and environmentally friendly photothermal heating materials and heterogeneous catalytic systems.

2. EXPERIMENTAL SECTION

2.1. Materials. Nitric acid, hydrochloric acid, 4-nitrophenol, trisodium citrate, KOH, isopropyl alcohol, hydrogen tetrachloroaurate-(III) trihydrate, and sodium borohydride (≥98%) were purchased from Fisher Scientific and used without purification. The water used for all reactions was obtained from a Nanopure Water System (Barnstead/Thermolyne). All glassware was cleaned with aqua regia, followed by treatment in a base bath, and then rinsed with water prior to use.

2.2. Preparation of Gold Nanoparticles under Daily Sunlight and Solar-Simulated Light. For the preparation of various sizes of gold nanoparticles by our photochemical reduction method, 0.2 mL of 1 wt % $HAuCl_4 \cdot 3H_2O$ solution was mixed with 10 mL of water in a 20 mL glass vial containing a magnetic stirring bar. Varying amounts (0.075−1.0 mL) of 1 wt % trisodium citrate were then introduced into the gold solution. The mixture was exposed to a solar-simulated light (providing ∼100 mW/cm^2, ∼5 cm in diameter, a continuous Xe arc lamp equipped with an optical filter, Newport Inc.) at room temperature for 90 min. The intensity of the light was closely adjusted to a condition of one-sun's solar radiation reaching the surface of the Earth,[34,35] allowing for our synthetic process to be tested with daily sunlight irradiation. Thus, a series of reaction vials containing the same concentrations of gold and trisodium citrate were exposed to daily sunlight (whose intensity fluctuated from ∼55 to ∼80 mW/cm^2 as measured by an optical power meter at 0, 30, 60, 90, and 120 min) to monitor the formation of various gold nanoparticles. Generally, we found that the formation of gold nanoparticles was much faster and more reliable with the solar-simulated light system, presumably due to the intense and stable light source over the course of the reaction. After the reaction was complete, the final solutions were stored at room temperature without further purification prior to analysis and use.

2.3. Preparation of Gold Nanoparticle Loaded Filter Paper. Clean filter papers (Whatman grade No. 1 filter paper, 55 mm) were initially dried in an oven at 50 °C overnight. Varying amounts (e.g., 1, 3, 5, 7, and 10 mL) of the prepared gold nanoparticles (∼35 nm in diameter) were then diluted with pure water to be 10 mL total volume in a glass Petri dish. The dried filter papers were immersed in the Petri dish (60 mm × 15 mm) containing different concentrations of gold nanoparticles (0.2−2.0 mg/10 mL) and were left for 24 h after covering the dish with a lid to minimize the evaporation of the water. The filter papers were then thoroughly rinsed with clean water and dried in the oven at 50 °C overnight. The initial and remaining gold solutions were subjected to absorption analysis by a UV−vis spectrophotometer to estimate the loading efficiency of the gold nanoparticles. We also attempted to compare the mass of the resulting filter papers to those of the initially dried filter papers using a ultramicrobalance (UMT2, Mettler Toledo), which did not provide us with a quantitative analysis. These gold-loaded filter papers were then employed in the photothermal heating and catalytic reduction of 4-nitrophenol under the solar-simulated light.

2.4. Photothermally Induced Heating and the Reduction of 4-Nitrophenol (4-NP) Using Gold-Nanoparticle-Loaded Filter Papers in the Presence and Absence of the Solar-Simulated Light..[3,27,36−38] Prior to the catalytic reduction of 4-NP, the gold-nanoparticle-loaded filter papers were briefly rinsed with pure water. Water (13.5 mL) and 4-nitrophenol (4-NP, 0.86 mL, 1 mM) were initially mixed in a 20 mL glass vial. $NaBH_4$ (0.86 mL, 0.1 M) was then added to the solution, resulting in a color change from colorless to bright yellow. This mixture solution was slowly transferred onto a gold-nanoparticle-loaded filter paper, which was already placed in the filtration system equipped with a 47 mm fritted disk. The catalytic reduction of 4-NP was carried out with and without the irradiation of the solar-simulated light (providing ∼100 mW/cm^2). The absorption bands of the initial solution and the aliquots collected after each filtration step were immediately recorded using a UV−vis spectrophotometer in the range of 200−1100 nm.

Similarly, a gold-nanoparticle-loaded filter paper was placed in a plastic dish containing the same amounts of water, 4-NP, and $NaBH_4$ as above, and the reduction reaction was subsequently performed with and without the solar-simulated light. The absorption bands of an aliquot of solution (0.10 mL) were recorded as a function of time. Each data point collected is the average of the minimum three trials. The temperature profiles of the gold-loaded filter paper containing the mixture solution and pure water (15 mL in a plastic dish) were also examined by an infrared thermal image analyzer. An additional control experiment was performed with a bare filter paper using the same amounts of 4-NP and $NaBH_4$ under the light irradiation, but no photoinduced reduction and/or degradation of 4-NP was observed even after 3 h of irradiation.

2.5. Characterization Method. To characterize the morphology, hydrodynamic diameter, and optical property of the gold nanoparticles, we employed a combination of scanning/transmission electron microscopy (SEM/TEM), dynamic light scattering (DLS), and UV−vis spectroscopy. An infrared thermal image analyzer was used to monitor the photothermal heating property of the gold-nanoparticle-loaded filter papers.

An FEI-Quanta 450 instrument, operating at 20 kV, was used to analyze the general size distribution and to evaluate the overall morphology of the gold nanoparticles. All samples were deposited from the solution onto silicon wafers or filter papers and then completely dried at room temperature overnight. The samples on the filter papers were coated with a thin gold film (~3 nm) using a Denton vacuum sputter coater (DESK II) to improve the electrical conductivity for imaging prior to analysis. TEM analysis was also performed with a Hitachi H8100 microscope operating at an accelerating voltage of 200 kV. An aqueous solution of gold nanoparticles was deposited and dried on a 300-mesh carbon-coated copper grid before analysis. The image-based size analysis was completed with ImageJ software (v1.45s, National Institute of Health) counting over 50 particles.

A benchtop powder X-ray diffraction (PXRD) instrument with Cu Kα radiation (MiniFlex 600, Rigaku Corp.) was used to examine the crystalline structure of the representative gold nanoparticles on filter papers (scan rage 10°−90°, 0.02° steps, 5°/min).

Dynamic light scattering (DLS, ZetaPALS, Brookhaven Instruments Corp., Holtsville, NY) equipped with a 35 mW solid state laser (90° and 15° angular measurements) was used to measure the hydrodynamic diameter and polydispersity index (PDI) of the gold nanoparticles at 20 °C. All samples were diluted in pure water. The data were collected from an average of five measurements over 100 s.

To characterize the optical properties of the gold nanoparticles, an Agilent UV−visible spectrometer was used over the wavelength range of 200−1100 nm. All samples were prepared in pure water and transferred to a quartz submicro cell.

Real-time temperature profiles of all samples were collected on the basis of the average of the three measurements by an infrared thermal image analyzer (Fluka FLIR40, Global Test Supply) and a traceable double thermometer with computer output (Fisher Scientific). The intensity of the light sources was estimated by a hand-held optical power meter (1916-C power meter, Newport Inc.).

3. RESULTS AND DISCUSSION

On the basis of our previous fluorescent-light-induced synthetic approach,[20] the concentrations of gold ions and trisodium citrate were required to be higher than those of conventional thermal reduction conditions.[21,22] Here we demonstrated a simple photochemical reduction method to prepare various gold nanoparticles by utilizing broad solar-based light sources (i.e., solar-simulated light and daily sunlight) under the similar reaction conditions. The use of low concentrations of gold ions resulted in the significantly slower and less reproducible formation of the desired diameters of the gold nanoparticles, while the increased gold concentrations allowed for a faster and more reliable formation of the tunable diameters of the gold nanoparticles under the irradiation of the broad-band light. Table 1 summarizes the various reaction conditions and the resulting diameters of gold nanoparticles with their polydispersity index (PDI) values. The overall sizes of the gold nanoparticles ranging from ~10 to ~160 nm (estimated by imageJ software and DLS for PDI values) were tuned by varying the amount of 1 wt % trisodium citrate from 1.0 to 0.075 mL. The formation of these gold nanoparticles was also observed by the systematic changes of the initial/final solution colors[39] and the absorption band maxima (vide infra).

Figure 1 shows the digital photo and SEM/TEM images of the gold nanoparticles prepared by the irradiation with a solar-simulated light (~100 mW/cm^2) for 90 min. These images clearly support the idea that various sizes of gold nanoparticles can be formed simply by adjusting the concentration of trisodium citrate in a fixed amount of aqueous $HAuCl_4 \cdot 3H_2O$ solution. Under our solar-simulated light-induced reaction conditions, uniform gold nanoparticles between 10 and 15 nm in diameter were typically formed and exhibited an almost similar solution color when an amount of citrate ≥0.50 mL was introduced into 10 mL of 0.02 wt % $HAuCl_4$. The TEM images exhibit a somewhat crystalline structure, and the selected area diffraction pattern of representative nanoparticles shows slightly broken rings with diffraction points, implying polycrystalline gold features in Figure S1 of the Supporting Information. When a lower volume of citrate (ranging from 0.40 to 0.075 mL) was added, the diameters of the nanoparticles systematically increased along with the distinctive solution color changes (Figure 1f). It is worthy to note that the use of trisodium citrate between 0.090 and 0.075 mL often led to the slightly less reproducible formation of large gold nanoparticles (e.g., >100 nm in diameter), which is also observed from conventional thermal reduction conditions.[12,13,21] Lastly, the addition of below 0.075 mL of trisodium citrate often failed to form gold nanoparticles or display any notable color changes, and prolonged light irradiation still did not result in the formation of gold nanoparticles. On the basis of these reaction conditions, we found that our photochemical reduction process utilizing the solar-simulated light readily allowed for the formation of gold nanoparticles ranging from 10 to 160 nm in diameter at room temperature.

Table 1. Photochemical Reaction Conditions To Prepare Various Gold Nanoparticles under the Irradiation of Solar-Based Light Sources

	0.2 mL of 1 wt % $HAuCl_4 \cdot 3H_3O$ in 10 mL of water		
		diameter in nm (PDI)	
1 wt % trisodium citrate (mL)	notable solution color change (min)	solar-simulated light	sunlight
1.0	≤3	~11 (0.15)	~10 (0.15)
0.50	~ 3	~13(0.16)	~10(0.16)
0.40	~ 4	~20 (0.09)	~18(0.11)
0.30	~ 5	~35 (0.10)	~27 (0.13)
0.20	~ 15	~70 (0.16)	~55 (0.19)
0.10	~ 23	~95 (0.20)	~78 (0.25)
0.090	~ 30	~115 (0.22)	~90 (0.29)
0.075	~ 35	~160 (0.25)	~100 (0.32)
<0.075	>45	partial aggregates	

Figure 2 presents the UV−vis absorption spectra of various gold nanoparticles prepared by solar-simulated light irradiation. Although most of the gold nanoparticle formation was accomplished within 60 min, the reaction mixtures were exposed to the light for 90 min to ensure the completion of the reactions; the completion of the reaction was proved both by the negligible increase of the maximum absorption bands of the gold nanoparticles and the disappearance of the gold ion peaks below 300 nm (see details of the reaction kinetics in Figure 2S of the Supporting Information).[11,20,40,41] As the position of the maximum absorption band is highly sensitive to the size of the gold nanoparticles,[13,39] the gradual red-shift and broadness of the absorption peaks around 520−600 nm corresponding to decreasing citrate volumes presumably indicate an overall increase in the size of the gold nanoparticles. These absorption patterns of the nanoparticles are relatively consistent with the results from the SEM/TEM images (although exhibiting the presence of a few aggregated gold nanoparticles) in Figure 1. When 1 wt % citrate was used at a volume of 0.50 mL or higher, the position of the absorption peak was negligibly changed, but the peak intensity centered at ~520 nm quickly increased,

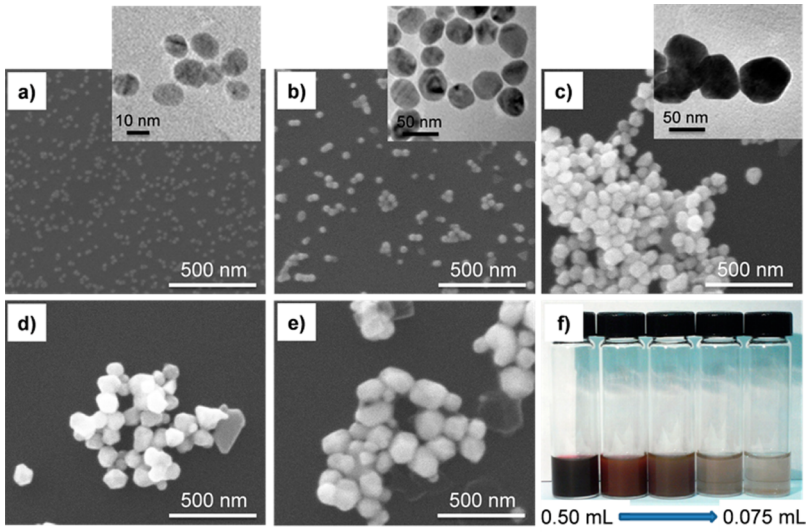

Figure 1. SEM/TEM images (a–e) and a digital photo (f) of gold nanoparticles prepared by varying amounts of 1 wt % trisodium citrate solution with 10 mL of 0.02 wt % gold solution under the irradiation of a solar-simulated light for 90 min: (a) 0.50 mL, (b) 0.30 mL, (c) 0.20 mL, (d) 0.10 mL, and (e) 0.075 mL of the citrate solution.

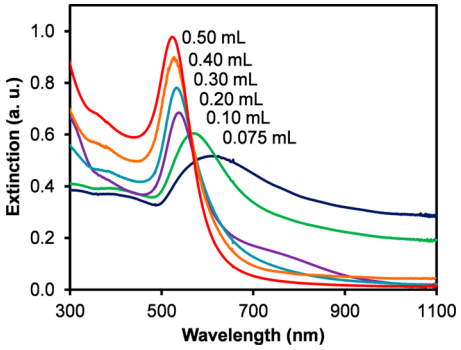

Figure 2. UV–vis absorption spectra of gold nanoparticles prepared by varying the amounts of 1 wt % trisodium citrate solution with a fixed amount of 0.02 wt % $HAuCl_4 \cdot 3H_2O$ solution under the solar-simulated light.

probably due to the rapid, increased number of small gold nanoparticle formation. The use of 1 wt % trisodium citrate below 0.075 mL, however, did not allow nanoparticles to develop notable absorption bands in the visible region, indicating incomplete reactions and/or severe aggregations. Extended light irradiation of the reaction mixture over 90 min still did not result in the formation of discrete nanoparticles but instead exhibited black precipitates or smeared gold films in the reaction flask caused by the photocoagulation of the gold particles (i.e., the photoneutralization process of the gold surface leading to aggregation).[42] Details of photoinduced (e.g., UV and visible light sources) formation and growth mechanism of metal nanoparticles can also be found in previous studies.[10,11,20,24,42,43] Overall, the systematic control of the gold nanoparticles with a relatively broad diameter range was accomplished with the gradual decrease of the amount of citrate

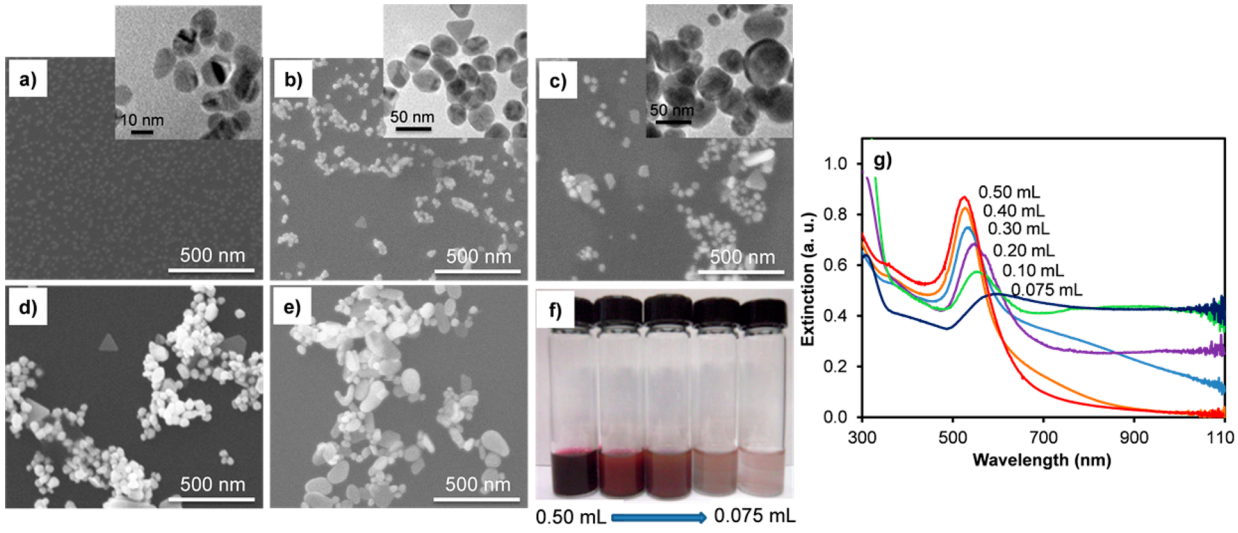

Figure 3. SEM/TEM images (a–e), a digital photo (f), and UV–vis absorption spectra (g) of gold nanoparticles prepared by varying amounts of 1 wt % trisodium citrate solution with a fixed amount of $HAuCl_4 \cdot 3H_2O$ solution (10 mL of 0.02 wt %) under the irradiation with sunlight for 150 min: (a) 0.50 mL, (b) 0.30 mL, (c) 0.20 mL, (d) 0.10 mL, and (e) 0.075 mL of citrate.

solution (0.075−0.5 mL) under the solar-simulated light irradiation.

The light-induced synthetic process for preparing gold nanoparticles involves the slow formation of a trace amount of gold seed particles upon the addition of a reducing agent (i.e., trisodium citrate) into a solution containing gold ions; the subsequent growth of the seed nanoparticles is enhanced by light irradiation,[11,20,43,44] Specifically, the formation of many gold seeds upon the addition of a high concentration of citrate is achieved at the beginning of the reaction (i.e., nucleation, which is elucidated by the notable solution color change from very pale yellow to light grayish purple that takes place under our reaction conditions; the data are summarized in Table 1). This is followed by the rapid growth of the seeds with the remaining gold ions under light irradiation, because the surface of these seed nanoparticles are reactive and serve as autocatalytic growth centers that promote the reduction of gold ions in the solution around the nanoparticles. In addition, when the typical absorption band of small gold seed nanoparticles falls in the wavelength of the incoming light source, it can rapidly enhance the growth of the nanoparticles. We expected that our overall photochemical process utilizing the high amount of trisodium citrate (e.g., 0.30 mL or higher) completed the reactions quickly and caused the formation of relatively small gold nanoparticles with narrow size distributions. When the amounts of trisodium citrate decreased (e.g., 0.075 and 0.090 mL of 1 wt % citrate), relatively slow development of absorption band of gold nanoparticles in the visible range and their notable color changes clearly implied the slow formation and growth of the seeds under light irradiation. This observation was probably due to the formation of a few gold seeds exhibiting a weaker absorption band at the beginning of the reaction, followed by the slightly slow growth process resulting in the formation of larger gold nanoparticles. A further decrease in the citrate amount (e.g., <0.075 mL) significantly slowed the overall reactions and caused the severe light-induced aggregation of the gold nanoparticles.

As our solar-simulated light source successfully induced the formation of various gold nanoparticles, we then employed daily sunlight in the preparation of the gold nanoparticles. Figure 3 shows the digital photo, SEM/TEM images, and absorption spectra of the gold nanoparticles prepared by irradiation with sunlight for 150 min. As the intensity of sunlight was measured to be 55−80 mW/cm^2, which was a little lower than the solar-simulated light, the reaction took slightly longer to complete the nanoparticle formation. Various sizes of gold nanoparticles (10−100 nm in diameter) were again formed by controlling the amount of 1 wt % citrate (Table 1). As speculated, use of real sunlight and varying amounts of trisodium citrate induced the distinctive solution colors (Figure 3f), which also implied the formation of different sizes of gold nanoparticles (confirmed by the absorption patterns in Figure 3g). The use of low citrate volumes (≤0.10 mL) often led to the formation of very polydisperse and nonspherical nanoparticles with some partial aggregations examined by the appearance of broad shoulder peaks above 650 nm.[45,46] Incomplete formation of gold nanoparticles was also observed by the presence of the residual gold ion peak below 300 nm.[40,41] This experiment, however, clearly demonstrated the possibility of utilizing daily sunlight for the preparation of gold nanoparticles without any electrical thermal input. In our separate study, the formation of gold nanoparticles was attempted under the constant intensity of the solar-simulated light at ∼70 mW/cm^2 by simply adjusting the distance of the solution mixture and the light source. The formation of gold nanoparticles was comparable to that under sunlight irradiation, but these gold nanoparticles were more spherical and had low PDIs, presumably due to the minimal fluctuation of light intensity over the course of the reaction. A more thorough study is underway to understand the light-intensity-dependent structural changes of the gold nanoparticles.

As our previous study showed the practical use of gold nanoparticles as a catalyst in solution under the irradiation of a solar-simulated light, which exhibited enhanced catalytic activities due to their moderate heating of the solution temperature,[47] we attempted to utilize these gold nanoparticles on a paper-based substrate in the absence of a solvent as a highly efficient photothermal heating material and light-enhanced heterogeneous catalyst. To verify this idea, the gold nanoparticles (∼35 nm in diameter) were embedded onto a filter paper and initially subjected to the irradiation of a solar-simulated light (∼100 mW/cm^2) to examine their photothermal heating efficiency. Prior to evaluating the photothermal heating property of the gold-loaded filter papers as a function of the gold nanoparticle concentration, the amount of loaded nanoparticles on a filter paper was carefully examined by the following approach: Initially, the differences in the maximum intensities of the absorbance peaks of a gold nanoparticle solution at ∼530 nm before and after treatment of the filter papers were compared to the those of standard solutions of gold nanoparticles via the Beer−Lambert law (Figure 4).

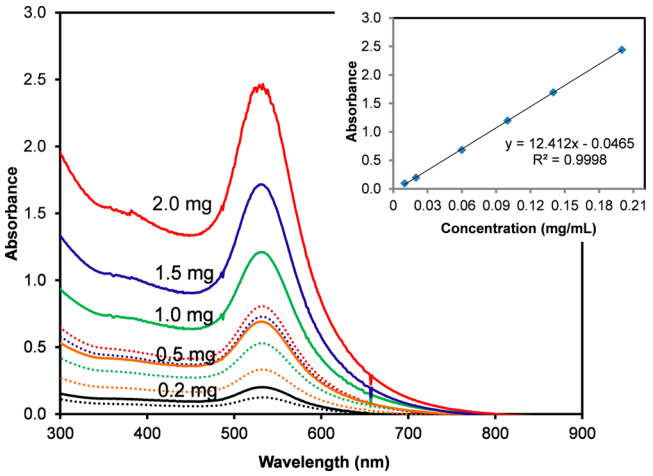

Figure 4. UV−vis absorption spectra of various concentrations of gold nanoparticle solutions (10 mL scale) before (solid lines) and after (dotted lines) treatment of the filter papers overnight. The inset represents the calibration curve for gold nanoparticle standards.

Overall, the total amount of gold nanoparticles loaded onto filter papers was systematically increased as a function of the initial gold nanoparticle concentration. These calculations were based on the following two assumptions: First, the reduction of gold ions to form gold particles resulted in a 100% conversion using our photochemical reaction method (see details in Figure S2 of the Supporting Information). Second, there was no loss of gold nanoparticles during the purification of the filter paper (i.e., rising with water) after treatment with the gold nanoparticle solution.

SEM, digital photos, and IR thermal images were collected to examine these filter papers as a function of the gold

nanoparticle loading (Figure 5). The overall distribution of the loaded gold nanoparticles on a filter paper was easily observed

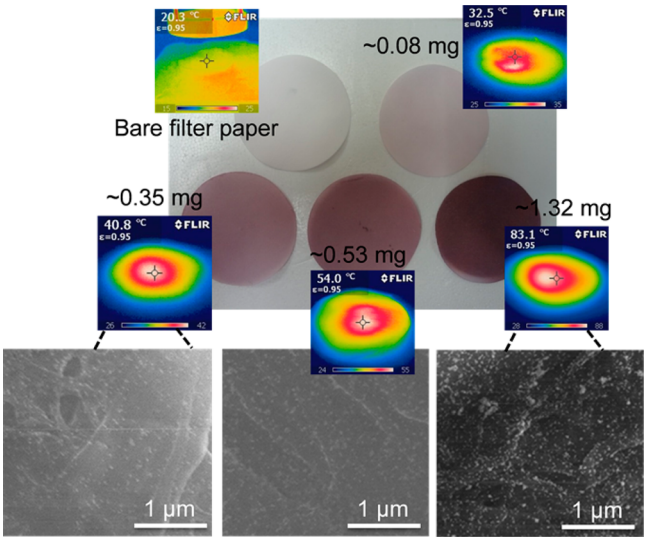

Figure 5. A digital photo, SEM images, and temperature profiles of bare and gold-nanoparticle-loaded filter papers measured by an IR-thermal camera.

in the SEM images. In addition, the powder X-ray diffraction (XRD) analysis in Figure S3 of the Supporting Information clearly supports the loading of crystalline gold nanoparticles on the filter-paper-based substrate. As the loading of the gold nanoparticles increased, the colors of the filter papers changed from light pink to dark purple (the digital photo in Figure 5). The IR thermal images evidently showed a systematic increase in the temperature profiles of the filter papers as a function of gold loading due to the efficient photothermal heating property of gold nanoparticles under light irradiation. The heating mechanism is simply explained: the strong interactions between the electric field of incident light and the collective oscillation of delocalized conduction electrons (i.e., SPR) of nanoscale metal particles result in the energy gain.[48,49] The gained energy then turns into heat that diffuses away from the nanoparticles, leading to a significant increase in the temperature in the vicinity of the nanoparticles and surrounding medium. It is also important to note that heat generation becomes strong when the wavelength of the incident light source is well-matched with the SPRs of the metal nanoparticles. Upon irradiation with the solar-simulated light for 3 min, a bare filter paper increased the temperature to ~28 °C and the gold-loaded filter papers increased the temperature to ~35 °C for 0.08 mg, ~42 °C for 0.35 mg, ~55 °C for 0.53 mg, ~68 °C for 0.80 mg, and ~88 °C for ~1.32 mg of gold nanoparticles. This apparent increase in the temperature under the broad-band solar-simulated light source was attributed to the photothermal heating property of the loaded gold nanoparticles possessing a strong SPR in the visible range.

The enhanced photothermal heating process by gold nanoparticles has been explained by the following two events:[49−51] First, the accumulative effect involves the addition of heat fluxes by single nanoparticles and more nanoparticles induce a stronger temperature increase.[50] Second, the Coulomb interaction is related to the interparticle distance and nanoparticle arrangements affecting the total heat generation.[51] The different amounts of heat generation between the two interacting nanoparticles and two individual nanoparticles are possibly attributed to the coupling of the SPR and the different rates of the heat dissipation process (caused by the interparticle Coulomb interaction). For example, shorter interparticle distances induce stronger SPR coupling and greatly affect the total heat generation (i.e., higher temperature).[49,51] These collective effects strongly impact the systematic increase in the temperature profiles of our gold-loaded filter papers (i.e., possibly increasing clustering/grouping of gold nanoparticles on the substrate) as a function of the nanoparticle concentration. We believe that the substrate-supported gold nanoparticles can take advantage of these effects—particularly the Coulomb interaction—much more efficiently than the nanoparticles in the solution. As the gold-loaded filter papers exhibited a significant, rapid increase in temperature under the irradiation of the solar-simulated light, we attempted to utilize them as substrate-supported heterogeneous catalysts because the efficiency of many chemical reactions can easily be affected by the reaction temperature. In addition, the loaded gold nanoparticles acting as heterogeneous catalysts on paper-based

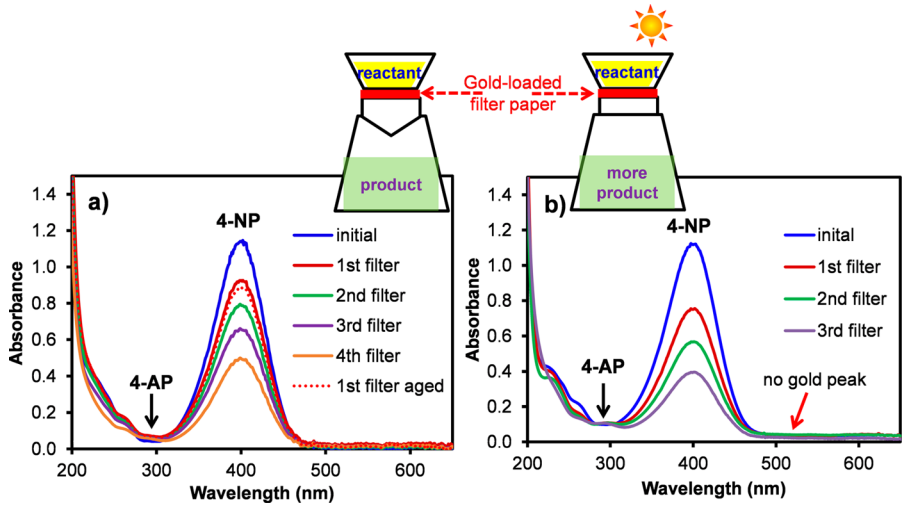

Figure 6. Absorption patterns of 4-NP upon filtration through the gold-nanoparticle-loaded filter paper (a) without and (b) with the irradiation of solar-simulated light.

substrates significantly minimize the light-induced coagulation process that often takes place during the solution-based chemical reactions.

As proof of the concept, the gold-loaded filter papers were subsequently tested as heterogeneous catalysts for the reduction of 4-nitrophenol (4-NP) to 4-aminophenol (4-AP) with and without solar-simulated light irradiation. As the mixture of 4-NP and sodium borohydride in an aqueous solution initially exhibited a strong absorption band at 400 nm (4-nitrophenolate ion) and the reduced 4-aminophenolate in the solution appears at 300 nm, the catalytic activities of the gold-nanoparticle-loaded filter papers can be simply monitored by these two absorption bands of the solution before and after each filtration step. We primarily compared the reduction of 4-NP using various gold-loaded filter papers in the presence and absence of the solar-simulated light; the filter papers with ∼0.35 and ∼0.53 mg of gold nanoparticles exhibited markedly different reduction rates of 4-NP upon filtration, unlike other gold-loaded filter papers. Specifically, the 4-NP reduction with the filter papers containing low amounts of gold nanoparticles (e.g., ∼0.08 mg) under light irradiation showed a slightly faster rate than those without light irradiation, presumably due to the low/moderate photothermal heating property. When a large number of gold nanoparticles loaded onto filter papers (e.g., ∼1.32 mg) were used for the 4-NP reduction with and without light irradiation, both reactions went notably fast because the reduction was mainly affected by the concentration of the loaded gold nanoparticles rather than the photothermal heating property.

Figure 6 shows two representative absorption band patterns of the 4-NP solution upon filtration using filter paper loaded with ∼0.53 mg of gold nanoparticles with and without the irradiation of solar-simulated light. As the number of filtration steps increased, the intensity at 400 nm for 4-NP notably decreased and a new peak at 300 nm appeared (or slightly increased), clearly indicating the formation of 4-AP. Under the light irradiation, a greater decrease of the absorption bands at 400 nm after each filtration step was observed, apparently caused by the photothermal heating of the loaded gold nanoparticles on the filter paper. To verify the photothermally enhanced reduction of 4-NP, two filter papers were loaded with the same concentration of the gold nanoparticle solution and subjected to both reactions without and with light irradiation. A gold-loaded filter paper was used in the reduction of 4-NP without light irradiation, followed by the reduction with light irradiation. The other filter paper was used for the reduction of 4-NP with light irradiation first, followed by the reduction without light irradiation. These filter papers were then dried in an oven overnight, transposed, and subjected to the second reduction after examining photothermal heating properties. It is also worth noting that the flow rate of the reaction solution was slightly faster under the light irradiation condition (more gold-loaded filter papers exhibited slightly faster flow), but still more reduction of 4-NP was observed from our simple filtration-based catalytic system. On the basis of these experiments and observations, we confirmed that the overall fast reduction of 4-NP upon filtration under the light irradiation was mainly caused by the photothermal heating property of the gold nanoparticles. More thorough studies including the flow-rate measurements of reaction solution using various filter papers as a function of gold nanoparticle loading with and without light irradiation and flow-rate-dependent catalytic reactions using a syringe pump are underway. Additionally, individual gold-loaded filter papers exhibited sustained catalytic activity through multiple trials, demonstrating their possible recyclability in catalytic reactions.

In our separate study, we investigated the possibility of gold nanoparticles leaching from the filter paper into the solution by the following method: the first filtrate solution was aged for 60 min, and we then measured the absorption band of 4-NP at 400 nm to examine the possible reduction of 4-NP by the leached gold nanoparticles. Interestingly, the negligible decrease of the 4-NP peak at 400 nm (dotted line in Figure 6a) suggested the absence of free gold nanoparticles in the filtrate solution, which was also confirmed by the undetectable absorption peak of the gold nanoparticles around 520−550 nm. Additionally, ICP-AES analysis (IRIS inductively coupled plasma-atomic emission spectroscopy, Thermo Jarrell Ash Corp.) did not show a noticeable concentration of gold atoms (i.e., ≤2.5 μg/mL) for various filtered solutions, strongly suggesting the spectroscopically negligible leaching of the gold nanoparticles during filtration. The photothermally induced temperature profiles of the filter papers before and after many filtrations remained similar, providing further indication of the insignificant leaching of the gold nanoparticles.

Furthermore, the gold-loaded filter papers were immersed in a solution containing 4-NP and $NaBH_4$ under solar-simulated light irradiation to monitor the reduction of 4-NP to 4-AP as a function of time (Figure 7 and the representative 4-NP

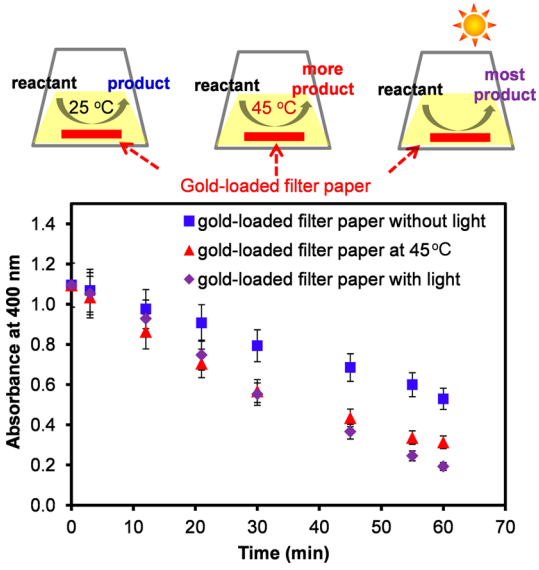

Figure 7. Absorption patterns of 4-NP in the presence of the gold-nanoparticle-loaded filter paper without (blue) and with (purple) the irradiation of solar-simulated light and the heated reaction solution at 45 °C (red).

reduction spectra in Figure S4 of the Supporting Information). Once more, the 4-NP reduction was completed much faster with the light irradiation than without the light source. After the complete reduction in 60 min with filter paper loaded with ∼0.53 mg of gold, the resulting solution temperature was ∼45 °C; this temperature was reached after the irradiation with light for ∼15 min. This fast reaction was clearly explained by the photothermal heating property of the loaded gold nanoparticles. These filter papers were placed in water over 60 min and did not show detectable leaching of the embedded gold nanoparticles (Figure S4 of the Supporting Information). Unlike the filtration method involving many filtration steps, this

approach allowed the 4-NP molecules to interact with the filter paper longer in the solution, which might be more efficient and convenient for catalytic reactions requiring an extended reaction time. In addition to the photothermal heating property, we attempted to evaluate if this fast reaction was also enhanced by the SPR of the gold nanoparticles. As such, the same reduction was performed with the gradual increase of the 4-NP solution's temperature (~45 °C) in the presence of the gold-loaded filter paper. This range of the temperature increase was similar to that range caused by the light-induced heating of the gold-loaded filter paper in solution. The reduction of 4-NP was still not fully completed in 60 min (red triangles in Figure 7); this reduction was slightly slower than that which occurred under the light irradiation conditions. This discrepancy may be attributed to the SPR-related enhancement, although it was difficult to conclude the exact influence of the SPR of the nanoparticles on the overall reaction based on such a short reduction process. It is also important to remember that the temperature of the gold-loaded filter paper surface under light irradiation is possibly higher than that of the solution,[31,48,52,53] which might also be attributed to the slightly faster reduction time. More thorough studies to examine the effect of SPR in chemical reactions are underway.

The advantages of paper-based heterogeneous catalytic systems include not only the use of the enhanced photothermal heating properties caused by the accumulative effect and the Coulomb interaction of gold nanoparticles under light irradiation but also the overall simple preparation/operation, cost-efficiency, environmental friendliness, and recyclability. Moreover, these types of catalytic systems do not require complicated purification steps before and after the chemical reactions. As a whole, the broad-band solar-based light sources can be utilized in both the preparation and applications of gold nanoparticles, which can lead to the development of practical photothermal heating materials and catalytic systems.

4. CONCLUSIONS

We demonstrated a reliable and cost-efficient method for preparing gold nanoparticles and their heterogeneous catalytic applications on a paper-based substrate under the irradiation of solar-based light sources. Thorough analyses by SEM, DLS, and UV−vis spectroscopy clearly presented the general size distribution and absorption properties of the gold nanoparticles. IR thermal camera images clearly illustrated the novel photothermal heating properties of these gold nanoparticles on a filter paper under light irradiation. Given this unique heating property, the highly enhanced 4-NP reduction with gold-loaded filter papers was observed in the presence of the solar-simulated light. The overall results collectively support the systematic formation of various gold nanoparticles and their improved photothermal heating properties, as well as the enhanced heterogeneous catalytic properties under the irradiation of solar-simulated light. As a whole, this novel strategy can be generalized for the preparation of various metallic nanoparticles and the design of simple catalytic systems that are practical and efficient under broad-band light irradiation.

■ ASSOCIATED CONTENT

Ⓢ Supporting Information

Selected area diffraction pattern, TEM, PXRD, and UV−vis are also provided to clarify the formation and catalytic activity of gold nanoparticles under the irradiation of solar-based light sources. This material is available free of charge via the Internet at http://pubs.acs.org.

■ AUTHOR INFORMATION

Corresponding Authors

*J.-H.K.: phone, 1-309-438-2604; e-mail, jkim5@ilstu.edu.
*H.B.: phone, 82-53-580-5569; e-mail, hsbyun@kmu.ac.kr.

Author Contributions

The manuscript was written through contributions of all authors. All authors have given approval to the final version of the manuscript.

Notes

The authors declare no competing financial interest.

■ ACKNOWLEDGMENTS

We gratefully acknowledge the financial support from the Department of Chemistry and the College of Arts and Sciences, Illinois State University. This research is also supported by Korea Ministry of Environment as "Global Top Project" (Project No: GT-14-B-01-002-0). The authors would like to thank Dr. Eirin Sullivan for assistance with the PXRD measurements.

■ REFERENCES

(1) *Nanoparticles and Catalysis*; Astruc, D., Ed. Wiley-VCH: New York, 2008.
(2) Guo, R.; Zhang, L.; Qian, H.; Li, R.; Jiang, X.; Liu, B. Multifunctional Nanocarriers for Cell Imaging, Drug Delivery, and Near-IR Photothermal Therapy. *Langmuir* **2010**, *26*, 5428−5434.
(3) Saha, S.; Pal, A.; Kundu, S.; Basu, S.; Pal, T. Photochemical Green Synthesis of Calcium-Alginate-Stabilized Ag and Au Nanoparticles and Their Catalytic Application to 4-Nitrophenol Reduction. *Langmuir* **2010**, *26*, 2885−2893.
(4) Lal, S.; Clare, S. E.; Halas, N. J. Nanoshell-Enabled Photothermal Cancer Therapy: Impending Clinical Impact. *Acc. Chem. Res.* **2008**, *41*, 1842−1851.
(5) Motl, N. E.; Smith, A. F.; DeSantis, C. J.; Skrabalak, S. E. Engineering Plasmonic Metal Colloids Through Composition and Structural Design. *Chem. Soc. Rev.* **2014**, *43*, 3823−3834.
(6) Jain, P. K.; Huang, X.; El-Sayed, I. H.; El-Sayed, M. A. Noble Metals on the Nanoscale: Optical and Photothermal Properties and Some Applications in Imaging, Sensing, Biology, and Medicine. *Acc. Chem. Res.* **2008**, *41*, 1578−1586.
(7) Huang, Y.; Wu, L.; Chen, X.; Bai, P.; Kim, D.-H. Synthesis of Anisotropic Concave Gold Nanocuboids with Distinctive Plasmonic Properties. *Chem. Mater.* **2013**, *25*, 2470−2475.
(8) Skrabalak, S. E.; Chen, J.; Sun, Y.; Lu, X.; Au, L.; Cobley, C. M.; Xia, Y. Gold Nanocages: Synthesis, Properties, and Applications. *Acc. Chem. Res.* **2008**, *41*, 1587−1595.
(9) Vaccarello, P.; Tran, L.; Meinen, J.; Kwon, C.; Abate, Y.; Shon, Y.-S. Characterization of Localized Surface Plasmon Resonance Transducers Produced from Au25 Nanoparticle Multilayers. *Colloids Surf., A* **2012**, *402*, 146−151.
(10) Xue, C.; Millstone, J. E.; Li, S.; Mirkin, C. A. Plasmon-Driven Synthesis of Triangular Core−Shell Nanoprisms from Gold Seeds. *Angew. Chem., Int. Ed.* **2007**, *46*, 8436−8439.
(11) Dong, S.; Tang, C.; Zhou, H.; Zhao, H. Photochemical Synthesis of Gold Nanoparticles by the Sunlight Radiation Using a Seeding Approach. *Gold Bull.* **2004**, *37*, 187−195.
(12) Kimling, J.; Maier, M.; Okenve, B.; Kotaidis, V.; Ballot, H.; Plech, A. Turkevich Method for Gold Nanoparticle Synthesis Revisited. *J. Phys. Chem. B* **2006**, *110*, 15700−15707.
(13) Link, S.; El-Sayed, M. A. Size and Temperature Dependence of the Plasmon Absorption of Colloidal Gold Nanoparticles. *J. Phys. Chem. B* **1999**, *103*, 4212−4216.

(14) Cole, J. R.; Mirin, N. A.; Knight, M. W.; Goodrich, G. P.; Halas, N. J. Photothermal Efficiencies of Nanoshells and Nanorods for Clinical Therapeutic Applications. *J. Phys. Chem. C* **2009**, *113*, 12090−12094.
(15) Storti, B.; Elisei, F.; Abbruzzetti, S.; Viappiani, C.; Latterini, L. One-Pot Synthesis of Gold Nanoshells with High Photon-to-Heat Conversion Efficiency. *J. Phys. Chem. C* **2009**, *113*, 7516−7521.
(16) Lukianova-Hleb, E. Y.; Lapotko, D. O. Influence of Transient Environmental Photothermal Effects on Optical Scattering by Gold Nanoparticles. *Nano Lett.* **2009**, *9*, 2160−2166.
(17) Ji, X.; Song, X.; Li, J.; Bai, Y.; Yang, W.; Peng, X. Size Control of Gold Nanocrystals in Citrate Reduction: The Third Role of Citrate. *J. Am. Chem. Soc.* **2007**, *129*, 13939−13948.
(18) Zhao, W.-B.; Zhu, J.-J.; Chen, H.-Y. Photochemical Synthesis of Au and Ag Nanowires on a Porous Aluminum Oxide Template. *J. Cryst. Growth* **2003**, *258*, 176−180.
(19) Sanchez-Gaytan, B. L.; Qian, Z.; Hastings, S. P.; Reca, M. L.; Fakhraai, Z.; Park, S.-J. Controlling the Topography and Surface Plasmon Resonance of Gold Nanoshells by a Templated Surfactant-Assisted Seed Growth Method. *J. Phys. Chem. C* **2013**, *117*, 8916−8923.
(20) Kim, J.-H.; Lavin, B. W.; Burnett, R. D.; Boote, B. W. Controlled Synthesis of Gold Nanoparticles by Fluorescent Light Rrradiation. *Nanotechnology* **2011**, *22*, 285602.
(21) Turkevich, J.; Stevenson, P. C.; Hilier, J. A Study of the Nucleation and Growth Processes in the Synthesis of Colloidal Gold. *Discuss. Faraday. Soc.* **1951**, *11*, 55−75.
(22) Frens, G. Controlled Nucleation for the Regulation of the Particle Size in Monodisperse Gold Suspensions. *Nature (London), Phys. Sci.* **1973**, *241*, 20−22.
(23) Kumar, S.; Gandhi, K. S.; Kumar, R. Modeling of Formation of Gold Nanoparticles by Citrate Method. *Ind. Eng. Chem. Res.* **2007**, *46*, 3128−3136.
(24) Mallick, K.; Wang, Z. L.; Pal, T. Seed-Mediated Successive Growth of Gold Particles Accomplished by UV Irradiation: A Photochemical Approach for Size-Controlled Synthesis. *J. Photochem. Photobiol., A* **2001**, *140*, 75−80.
(25) Cortie, M. B.; van der Lingen, E. Catalytic Gold Nanoparticles. *Mater. Forum* **2002**, *26*, 1−14.
(26) Han, J.; Guo, R. Facile Synthesis of Highly Stable Gold Nanoparticles and Their Unexpected Excellent Catalytic Activity for Suzuki−Miyaura Cross-Coupling Reaction in Water. *J. Am. Chem. Soc.* **2009**, *131*, 2060−2061.
(27) Zeng, J.; Zhag, Q.; Chen, J.; Xia, Y. A Comparison Study of the Catalytic Properties of Au-Based Nanocages, Nanoboxes, and Nanoparticles. *Nano Lett.* **2010**, *10*, 30−35.
(28) Zhu, H.; Ke, X.; Yang, X.; Sarina, S.; Liu, H. Reduction of Nitroaromatic Compounds on Supported Gold Nanoparticles by Visible and Ulitraviolet Light. *Angew. Chem., Int. Ed.* **2010**, *49*, 6957−9661.
(29) Sershen, S. R.; Westscott, S. L.; Halas, N. J. Temperature-Sensitive Polymer−Nanoshell Composites for Photothermally Modulated Drug Delivery. *J. Biomed. Mater. Res.* **2000**, *51*, 293−298.
(30) West, J. L.; Halas, N. J. Applications of Nanotechnology to Biotechnology: Commentary. *Curr. Opin. Biotechnol.* **2000**, *11*, 215−217.
(31) Maity, S.; Downen, L. N.; Bochinski, J. R.; Clarke, L. I. Embedded Metal Nanoparticles as Localized Heat Sources: An Alternative Processing Approach for Complex Polymeric Materials. *Polymer* **2011**, *52*, 1674−1685.
(32) Ngo, Y. H.; Li, D.; Simon, G. P.; Garnier, G. Gold Nanoparticle−Paper as a Three-Dimensional Surface Enhanced Raman Scattering Substrate. *Langmuir* **2012**, *28*, 8782−8790.
(33) Adleman, J. R.; Boyd, D. A.; Goodwin, D. G.; Psaltis, D. Heterogenous Catalysis Mediated by Plasmon Heating. *Nano Lett.* **2009**, *9*, 4417−4423.
(34) Gueymard, C.; Myers, D.; Emery, K. Proposed Reference Irradiance Spectra for Solar Energy Systems Testing. *Sol. Energy* **2002**, *73*, 443−467.
(35) Kamat, P. V. Quantum Dot Solar Cells. Semiconductor Nanocrystals as Light Harvesters. *J. Phys. Chem. C* **2008**, *112*, 18737−18753.
(36) Khalavka, Y.; Becker, J.; Sonnichsen, C. Synthesis of rod-shaped gold nanorattles with improved plasmon sensitivity and catalytic activity. *J. Am. Chem. Soc.* **2009**, *131*, 1871−1875.
(37) Lee, J.-S.; Park, J. C.; Song, H.; Nanoreactor, A. Framework of a Au@SiO_2 Yolk/Shell Structure for Catalytic Reduction of p-Nitrophenol. *Adv. Mater.* **2008**, *20*, 1523−1528.
(38) Panigrahi, S.; Basu, S.; Praharaj, S.; Pande, S.; Jana, S.; Pal, A.; Ghosh, S. K.; Pal, T. Synthesis and Size-Selective Catalysis by Supported Gold Nanoparticles: Study on Heterogeneous and Homogeneous Catalytic Process. *J. Phys. Chem. C* **2007**, *111*, 4596−4605.
(39) Underwood, S.; Mulvaney, P. Effect of the Solution Refractive Index on the Color of Gold Colloids. *Langmuir* **1994**, *10*, 3427−3430.
(40) Chakraborty, A.; Chakraborty, S.; Chaudhuri, B.; Bhattacharjee, S. Spectroscopic Estimation of Chloroauric Acid During Synthesis of Gold Nanoparticles by Citrate Reduction Method. *Adv. Sci. Eng. Med.* **2012**, *4*, 128−131.
(41) Liang, X.; Wang, Z.-J.; Liu, C.-J. Size-Controlled Synthesis of Colloidal Gold Nanoparticles at Room Temperature under the Influence of Glow Discharge. *Nanoscale Res. Lett.* **2010**, *5*, 124−129.
(42) Satoh, O.; Hasegawa, H.; Tsujii, K.; Kimura, K. Photoinduced Coagulation of Au Nanocolloids. *J. Phys. Chem.* **1994**, *98*, 2143−2147.
(43) Xue, C.; Metraux, G. S.; Millstone, J. E.; Mirkin, C. A. Mechanistic Study of Photomediated Triangluar Silver Nanoprism Growth. *J. Am. Chem. Soc.* **2008**, *130*, 8337−8344.
(44) Jin, R.; Cao, Y.; Mirkin, C. A.; Kelly, K. L.; Schatz, G. C.; Zheng, J. G. Photoinduced Conversion of Silver Nanosphere to Nanoprisms. *Science* **2001**, *294*, 1901−1903.
(45) Ghosh, S. K.; Pal, T. Interparticle Coupling Effect on the Surface Plasmon Resonance of Gold Nanoparticles: From Theory to Applications. *Chem. Rev.* **2007**, *107*, 4797−4862.
(46) Haiss, W.; Thanh, N. T. K.; Aveyard, J.; Fernig, D. G. Determination of Size and Concentration of Gold Nanoparticles from UV−Vis Spectra. *Anal. Chem.* **2007**, *79*, 4215−4221.
(47) Kim, J.-H.; Lavin, B. W.; Boote, B. W.; Pham, J. A. Photothermally Enhanced Catalytic Activity of Partially Aggregated Gold Nanoparticles. *J. Nanopart. Res.* **2012**, *14*, 955−964.
(48) Neumann, O.; Urban, A. S.; Day, J.; Lal, S.; Nordlander, P.; Halas, N. J. Solar Vapor Generation Enabled by Nanoparticles. *ACS Nano* **2013**, *7*, 42−49.
(49) Govorov, A. O.; Richardson, H. H. Generating Heat with Metal Nanoparticles. *Nano Today* **2007**, *2*, 30−38.
(50) Richardson, H. H.; Hickman, Z. N.; Govorov, A. O.; Thomas, A. C.; Zhang, W.; Kordesch, M. E. Thermooptical Properties of Gold Nanoparticles Embedded in Ice: Characterization of Heat Generation and Melting. *Nano Lett.* **2006**, *6*, 783−788.
(51) Govorov, A. O.; Zhang, W.; Skeini, T.; Richardson, H. H.; Lee, J.; Kotov, N. A. Gold Nanoparticle Ensembles as Heaters and Actuators: Melting and Collective Plasmon Resonances. *Nanoscale Res. Lett.* **2006**, *1*, 84−90.
(52) Maity, S.; Kozek, K. A.; Wu, W.-C.; Tracy, J. B.; Bochinski, J. R.; Clarke, L. I. Anisotropic Thermal Processsing of Polymer Nanocomposites via the Photothermal Effect of Gold Nanorods. *Part. Part. Syst. Charact.* **2013**, *30*, 193−202.
(53) Zedan, A. F.; Moussa, S.; Terner, J.; Atkinson, G.; El-Shall, M. S. Ultrasmall Gold Nanoparticles Anchored to Graphene and Enhanced Photothermal Effects by Laser Irradiation of Gold Nanostructures in Graphene Oxide Solutions. *ACS Nano* **2013**, *7*, 627−636.